Development 130, 2729-2739

doi:10.1242/dev.00474

Tbx5 and Tbx4 trigger limb initiation through activation of the Wnt/Fgf signaling cascade

Jun K. Takeuchi*, Kazuko Koshiba-Takeuchi*, Takayuki Suzuki, Mika Kamimura, Keiko Ogura and Toshihiko Ogura†

Graduate School of Biological Sciences, Nara Institute of Science and Technology, 8916-5, Takayama, Ikoma, Nara 630-0101, Japan

*Present address: Cardiovascular Research, The Hospital for Sick Children, 555 University Avenue, Toronto, ON M5G 1X8, Canada
†Author for correspondence (e-mail: ogura@bs.aist-nara.ac.jp).

Accepted 24 February 2003

SUMMARY

A tight loop between members of the fibroblast growth factor and the Wnt families plays a key role in the initiation of vertebrate limb development. We show for the first time that *Tbx5* and *Tbx4* are directly involved in this process. When dominant-negative forms of these Tbx genes were misexpressed in the chick prospective limb fields, a limbless phenotype arose with repression of both Wnt and Fgf genes By contrast, when *Tbx5* and *Tbx4* were misexpressed in the flank, an additional wing-like and an additional leg-like limbs were induced, respectively. This additional limb formation was accompanied by the induction of both Wnt and Fgf genes These results highlight the pivotal roles of *Tbx5* and *Tbx4* during limb initiation, specification of forelimb/hindlimb and evolution of tetrapod limbs, placing Tbx genes at the center of a highly conserved genetic program.

Key words: Tbx5, Tbx4, Limb initiation, Wnt, Fgf, Chick

INTRODUCTION

T-box (Tbx) genes play key roles during organogenesis and pattern formation in both vertebrate and invertebrate embryos. They encode a group of transcription factors characterized by a highly conserved DNA-binding motif (T-box) and its unusual mode of DNA recognition (Kispert and Herrmann, 1993; Muller and Herrmann, 1997). From a combination of embryological and genetic approaches, a picture is emerging that Tbx genes belong to highly conserved genetic networks (Papaioannou and Silver, 1998; Smith, 1999; Ruvinsky and Gibson-Brown, 2000; Tada and Smith, 2001). Among Tbx genes, the best characterized are *Tbx5* and *Tbx4* (Chapman et al., 1996; Gibson-Brown et al., 1996; Ohuchi et al., 1998; Gibson-Brown et al., 1998; Issac et al., 1998; Logan et al., 1998). *Tbx4* is expressed in the developing hindlimb bud, whereas *Tbx5* is expressed in the forelimb, heart, and dorsal side of the retina. Previous studies have shown that *Tbx5* induces wing-like morphological changes in the chick leg when misexpressed in early developmental stages. By contrast, *Tbx4* induces leg-like alterations in the chick wing. These data indicate that *Tbx5* and *Tbx4* are involved in the specification of hindlimb/forelimb identity (Rodrigues-Esteban et al., 1999; Takeuchi et al., 1999). We have shown that *Tbx5* and *Tbx4* expression occurs even before the initiation of limb outgrowth. This evidence suggests that these two Tbx genes are directly involved in both the processes of limb initiation at early stages and in the specification of limb identity at later stages, highlighting their multiple roles.

Recent studies have shown that members of the fibroblast growth factor (Fgf) family play key roles in the limb initiation (Martin, 1998; Martin, 2001). When applied locally in the lateral plate mesoderm, several Fgfs induce an ectopic limb (Cohn et al., 1995; Ohuchi et al., 1995; Crossley et al., 1996; Vogel et al., 1996; Ohuchi et al., 1997). In a current model, signaling of two different Fgfs, Fgf8 and Fgf10, is a key for the limb outgrowth (Martin, 2001). Although data highlight the pivotal roles of Fgfs, limb bud formation is initiated in *Fgf10* knockout mice, suggesting that another factor(s) may induce limb initiation (Sekine et al., 1999; Min et al., 1998). Interestingly, limb buds of the *Fgf10*-null mice exhibit robust expression of *Tbx5* and *Tbx4* in the limb fields, although the limb buds cease to grow and remain flat (Sekine et al., 1999; Min et al., 1998). This observation indicates that *Tbx5* and *Tbx4* may be constituents of the a priori genetic program that acts upstream of the Fgf signaling cascade.

Recently, tight crosstalk between Fgf and Wnt proteins, another family of secreted factors, has been shown to control limb initiation in the chick embryo (Kawakami et al., 2001). *Wnt2b* and *Wnt8c* (which are expressed in the chick forelimb and hindlimb, respectively) are capable of inducing ectopic limbs in the flank. This additional limb formation is mediated through a β-catenin-dependent process and subsequent *Fgf10* induction, placing Wnt proteins upstream of Fgf signaling. However, the intracellular events that control expression and signaling of these extracellular factors have not been elucidated. To date, Hox9 genes are known to be expressed in the lateral plate mesoderm and to demarcate the normal limb

fields and the Fgf-induced additional limbs. This indicates that the Hox code, along the anteroposterior axis of the embryo, is one of the key determinants for the limb bud fields, implying that Hox genes act upstream of these signaling molecules (Cohn et al., 1997). Nonetheless, there is a gap between the Hox genes and the Wnt/Fgf network, in which putative transcription factor(s) act as initiator(s) of limb bud development. To explore this, we performed a series of experiments using both loss-of-function and gain-of-function approaches. Our data highlight the pivotal roles played by *Tbx5* and *Tbx4* during initiation of limb bud outgrowth.

MATERIALS AND METHODS

Chick embryos

Fertilized chick eggs were purchased from Takeuchi and Yamagishi poultry farms (Nara, Japan). Eggs were incubated at 39°C in a humidified incubator, and embryos were staged as described (Hamburger and Hamilton, 1951). Embryos were fixed in 4% paraformaldehyde (PFA) at 4°C overnight, washed three times, dehydrated with graded methanol, and then stored in 100% methanol at –30°C. To stain the skeletal elements, embryos were fixed in 5% Trichloroacetic acid (TCA) and stained with 0.1% Alcian Blue.

Plasmids construction

The coding regions of chick *Tbx5* and *Tbx4* were amplified by the PCR, and ligated into a pSLAX 12 Nco vectors (pSLAX-*Tbx5* and *Tbx4*, respectively) (Mogan and Fekete, 1996). To construct the dominant-negative forms, a repressor domain of the *Drosophila Engrailed* gene (Jaynes and O'Farrell, 1991) was ligated into the pSLAX plasmid (pSLAX-*En*). Entire sequences of chick *Tbx5* and *Tbx4* were amplified by the PCR with primers, then ligated to pSLAX-*En* to create fusion genes (pSLAX-*EnTbx5* and pSLAX-*EnTbx4*). In both cases, *En* gene was placed at the N termini. These fusion cDNAs were isolated and subcloned into a RCASBP retroviral vector and a modified pCAGGS vector (Niwa et al., 1991; Koshiba-Takeuchi et al., 2000).

Retrovirus preparation and injection

RCASBP-*EnTbx5* and *EnTbx4* plasmids were transfected into chick embryonic fibroblast cells isolated from SPF chick embryo (line c/o) trunks, then cultured for 1 week to allow the virus to spread. Cells were replaced with low-serum media, and incubated further for virion production. Then, media were collected and spun to concentrate virus particles as previously described (Morgan and Fekete, 1996).

The concentrated virus solution was mixed with an indicator dye (Fast Green), and injected into the prospective wing and leg fields.

In ovo electroporation

In ovo electroporation was carried out as previously described (Takeuchi et al., 1999; Momose et al., 1999). We modified our in ovo electroporation techniques to obtain efficient expression of the transgenes in the limb buds. Briefly, a CUY-21 electroporator (Gene System, Osaka, Japan) was used. Two platinum electrodes (Gene System, Osaka, Japan) were used. An anode was inserted beneath the embryonic endoderm and a cathode was placed on the ectoderm surface. Then, a DNA solution was injected by a sharp glass pipette into the embryonic tissues. Electric pulses were applied (7-9 V, 60 mseconds pulse-on, 50 mseconds pulse-off, three to five times) during injection of the DNA solution.

Whole-mount in situ hybridization and probe isolation

In situ hybridization was performed as previously described (Wilkinson, 1993). Probes for chick *Wnt8c*, *Fgf10* and *Fgf8* were kindly provided by Drs Jane Dodd, Sumihare Noji and Juan Carlos Izpisua Belmonte (Hume and Dodd, 1993; Vogel et al., 1996; Ohuchi et al., 1997). Chick *Pea3* was amplified by RT-PCR utilizing the published sequence, then subcloned into the pKRX vector (Schutte et al., 1997). The DNA fragment encoding the *Env* gene was isolated from the RCASBP retrovirus vector (Mogan and Fekete, 1996), and then subcloned into pBluescript SKII(+) vector. Chick *Wnt2b* was also amplified by RT-PCR, then subcloned into the pKRX vector.

RESULTS

Misexpression of the dominant-negative *Tbx5* and *Tbx4* induces the limb-less phenotype

Data obtained from *Fgf10*-null mice suggest that *Tbx5* and *Tbx4* act upstream of *Fgf10* signaling (Sekine et al., 1999; Min et al., 1998). To confirm this in chick embryos, *Tbx5* and *Tbx4* dominant-negative forms were constructed by fusing the *Engrailed* suppressor domain to their N termini (*EnTbx5* and *EnTbx4*, respectively) (Jaynes and O'Farrell, 1991). When increasing amounts of these fusion proteins were introduced into cultured limb mesenchyme cells along with the *Anf* (*atrial natriuretic factor*) promoter-luciferase (Hiroi et al., 2001; Bruneau et al., 2001) or mouse *Fgf10* promoter-luciferase reporter (a kind gift from Dr B. Bruneau), *EnTbx5* and *EnTbx4* repressed *Tbx5*- and *Tbx4*-dependent transactivation of these reporters, respectively, in a dose-dependent manner (data not shown). This suggests that the repressive action of the *Engrailed* suppressor domain, which was reported to be mediated through interaction with Groucho (Jimenez et al., 1997; Tolkunova et al., 1998), functions in the mesenchyme cells of limb bud. We inserted these fusion constructs into an RCAS retroviral vector and prepared infectious virions from chick embryonic fibroblast cells (Mogan and Fekete, 1996).

When the *EnTbx5* retrovirus was infected into the right prospective wing field at stages 7 to 10, a completely wingless phenotype arose at E12 (Fig. 1A). As expected, wing formation was completely disturbed at the shoulder level (Fig. 1A′): the right scapula is missing, leaving hypomorphic ribs underneath (red arrowheads in Fig. 1A′). In some cases, severe distal truncation was observed at E9 (Fig. 1B). Embryo skeletal preparations showed truncated wings (W′) with hypoplastic scapular (s′) and clavicular bones (c′) (Fig. 1B′).

When *EnTbx4* was misexpressed in the right prospective leg field, two phenotypes were obtained. Infection at the early stages (stage 7 to 10) resulted in a completely legless phenotype (red arrowheads in Fig. 1C,C′). In this embryo, hypoplastic ilium and ischium were evident (il′ and is′ in Fig. 1C′, respectively). The pubis was absent, making the right side of the pelvis hypoplastic and deformed (Fig. 1C′).

When the *EnTbx4* viral infection was performed at later stages (stage 11 to 13), the legless phenotype was not obtained, instead leg structure truncation occurred (red arrowheads in Fig. 1D). In this case, the right leg was small and severely distorted, as observed by Alcian Blue staining (red arrowhead in Fig. 1D′): a short and thin femur (f′ in Fig. 1D′) and hypomorphic distal structures (red arrowheads in Fig. 1D′). In addition, the right ilium and ischium were small and deformed (il′ and is′ in Fig. 1D′, respectively), and the pubis was missing from the pelvis right side (Fig. 1D′). These results indicate that *Tbx5* and *Tbx4* are directly involved in limb formation processes.

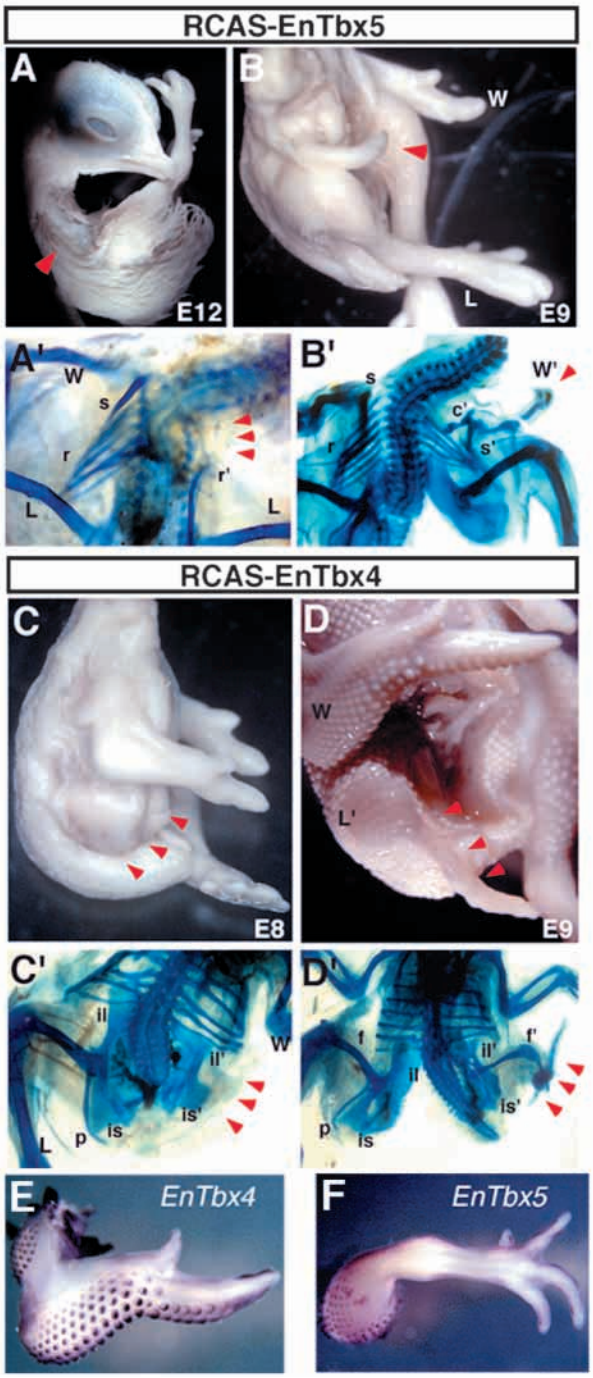

Fig. 1. Misexpression of dominant-negative Tbx genes induces a limbless phenotype. (A) When dominant-negative *Tbx5* (*EnTbx5*) was misexpressed by retroviral infection at stages 7 to 10, a wingless phenotype (arrowhead) arose at E12. (A′) Skeletal examination of A revealed that wing formation was completely blocked. Legs (L) and the left wing (W) were normal. Formation of the right scapula was completely suppressed with hypoplastic ribs underneath (r′) (arrowheads). On the uninfected left side, normal scapula (s) and ribs (r) were evident. (B) In another case, severe distal truncation was obtained at E9 (indicated by a red arrowhead), although this embryo showed normal morphology in the legs (L) and left wing (W). (B′) Skeletal examination of B showed truncated wing (W′) with hypoplastic scapula (s′) and clavicula (c′). In both cases, shoulders were hypomorphic. (C) When dominant-negative *Tbx4* (*EnTbx4*) was similarly misexpressed, a legless phenotype was observed at E8 (red arrowheads). (C′) Skeletal preparation of C. Right leg was specifically affected (red arrowheads). Right wing (W) and left leg (L) were normal. This embryo showed the hypomorphic ilium (il′) and ischium (is′) without pubis formation, making the right side of the pelvis deformed and hypoplastic (red arrowheads). In the left leg (L), normal ilium (il), ischium (is), and pubis (p) were formed. (D) When *EnTbx4* viral infection was performed at later stages (11 to 13), truncation of leg (L′) structures arose (red arrowheads) with normal wing formation (W). (D′) Skeletal preparation of (D) showed a severely distorted leg (red arrowheads). Hypomorphic ilium (il′), ischium (is′), and femur (f′) were evident with truncated distal structures (red arrowheads). In this side, the pubis was missing, although femur (f), ilium (il), ischium (is) and pubis (p) were normally formed on the uninfected left side. (E) Misexpression of *EnTbx4* in the wing did not induce morphological alteration at E8, although whole-mount in situ hybridization using *Env* gene in the RCAS vector indicate expression of *Tbx4* transgene. (F) Likewise, misexpression of EnTbx5 resulted in normal morphology in the leg, despite of the *Env* expression.

To examine the specificity of *EnTbx5* and *EnTbx4*, we misexpressed these genes in leg and wing buds, respectively. Misexpression of *EnTbx4* in the wing bud and *EnTbx5* in the leg did not induce any morphological abnormality at E8 (Fig. 1E,F, respectively). Whole-mount in situ hybridization for the *Env* gene encoded in the vector revealed expression of transgenes in limbs (Fig. 1E,F). Although signals were observed only on the limb surface, expression of transgenes and the resultant normal morphology suggest that *EnTbx5* and *EnTbx4* specifically abrogate development of the wing and leg buds, respectively.

Stage-dependent action of the dominant-negative *Tbx5* and *Tbx4*

In a series of misexpression studies, the resultant phenotypes are dependent on viral infection timing. To explore further, we injected dominant-negative Tbx viruses at various developmental stages that included stages 7 to 13 (Table 1).

Interestingly, limbless phenotypes were obtained only when the viruses were injected between stages 7 and 10. Viral injection at later stages (10 to 13) failed to induce any limbless alterations, setting up a short critical period. As there is a lag between viral injection and full transgene expression in the RCAS vector, viral injection between stages 7 and 10 results in the full expression of *EnTx5* and *EnTbx4* in stages 11 to 14 (Mogan and Fekete, 1996). As previously reported, the crosstalk between Wnts and Fgfs and the subsequent limb induction process begin around stage 14 (Kawakami et al., 2001). This implies that early viral injection and subsequent expression of dominant-negative Tbx genes may affect processes that precede the Wnts and Fgfs interaction, highlighting the putative roles of Tbx genes in limb initiation, rather than in limb outgrowth maintenance. By contrast, limb truncation occurred even in the cases of later viral infection, although the ratio decreases as the limb development proceeds. This suggests that the dominant-negative Tbx expression at later stages only weakly affect the maintenance phase, in which the Wnt and Fgf signaling cascades primarily operate. Nonetheless, we cannot exclude the possibility that lower

Table 1. Stage-dependent actions of the dominant-negative *Tbx5* and *Tbx4*

A Effect of misexpression *RCAS-EnTbx5*

Stage of infection	Total	Number with wingless phenotype	Number with wing truncations
7	10	7 (70%)	2 (20%)
8	15	12 (80%)	2 (13%)
9	12	8 (67%)	3 (25%)
10	13	3 (23%)	5 (38%)
11	9	0 (0%)	2 (22%)
12	11	0 (0%)	1 (9%)
13	10	0 (0%)	1 (10%)
Totals	80	30	16

Stage of infection	Total	Number with legless phenotype	Number with leg truncations
8	6	0 (0%)	0 (0%)
9	11	0 (0%)	0 (0%)
11	12	0 (0%)	0 (0%)
13	7	0 (0%)	0 (0%)
Totals	36	0	0

B Effect of misexpression of *RCAS-EnTbx4*

Stage of infection	Total	Number with legless phenotype	Number with leg truncations
7	8	6 (75%)	2 (25%)
8	18	11 (61%)	5 (28%)
9	12	8 (67%)	3 (33%)
10	13	2 (15%)	7 (54%)
11	12	0 (0%)	6 (50%)
12	14	0 (0%)	2 (14%)
13	15	0 (0%)	2 (13%)
Totals	92	27	27

Stage of infection	Total	Number with wingless phenotype	Number with wing truncations
8	5	0 (0%)	0 (0%)
9	16	0 (0%)	0 (0%)
11	10	0 (0%)	0 (0%)
13	5	0 (0%)	0 (0%)
Totals	36	0	0

Wingless and legless phenotypes were obtained only when the viruses of the dominant-negative *Tbx5* (*EnTbx5*) and *Tbx4* (*EnTbx4*) were infected between stages 7 and 10. Viral injection at later stages (stage 10 to 13) induced limb truncation at a lower rate, revealing a critical period between stages 7 and 10. By contrast, misexpression of *EnTbx5* in the leg and *EnTbx4* in the wing did not induce morphological alteration even when infected at early stages.

infection rate in later stages prohibited wide spread of virus and suppressed appearance of the complete limbless phenotype, although we did not observe significant differences in the viral gene expression induced by the infection between stage 9 and 11.

As observed in Fig. 1E,F, misexpression of *EnTbx5* and *EnTbx4* in the leg and wing, respectively, did not induce the limbless or the limb truncation phenotype (Table 1). This again supports the specific actions of *EnTbx5* and *EnTbx4* in the developing limb buds.

Misexpression of the dominant-negative *Tbx5* and *Tbx4* represses the Wnt/Fgf signaling

Our data strongly suggest that *Tbx5* and *Tbx4* directly control limb initiation processes. To confirm this further, the expression of several genes in the *EnTbx5*- and *EnTbx4*-misexpressed limb buds was examined. In this case, the dominant-negative forms of *Tbx5* and *Tbx4* were misexpressed by in ovo electroporation, as the electroporation enables us to express two plasmids simultaneously. Consequently, we monitored the domains of transgene expression by co-electroporation of an *EGFP* (*enhanced green fluorescent protein*) expression plasmid (pCAGGS-*EGFP*) (Takeuchi et al., 1999; Momose et al., 1999).

When the dominant-negative *EnTbx5* was misexpressed in the right prospective wing field, *Wnt2b* was downregulated in a region where GFP signals were evident (Fig. 2A,A′). Normal expression of this gene was observed in the lateral plate mesoderm of the left wing field (Kawakami et al., 2001). By contrast, when electroporation was performed in the right prospective leg field, *Wnt8c* expression was normal in a GFP-positive area (Fig. 2B,B′) (Hume and Dodd, 1993), implying that *EnTbx5* misexpression specifically affects *Wnt2b* in the wing field, but not *Wnt8c* in the leg. When *Fgf8* expression was analyzed, this gene was repressed in the right limb buds (red arrowheads in Fig. 2C). Normal expression of *Fgf8* was evident in the AER on the contralateral side (Fig. 2C). As the *EnTbx5* fusion gene was inserted in the RCAS retrovirus vector, in situ hybridization utilizing an *Env* probe visualizes the transgene expression domain. Nineteen hours after electroporation, robust *Env* expression was detected at the prospective wing field (arrowheads in Fig. 2D), indicating successful *EnTbx5* misexpression in this area. As shown in serial sections, *Fgf10* expression was downregulated in the same region of the embryo (arrowheads in Fig. 2E). Next, chick *Pea3* expression was examined, as *Pea3* encodes an Ets-type transcription factor that acts downstream of Fgf signaling (Roehl and Nusslein-Volhard, 2001; Raible and Brand, 2001). As expected, *Pea3* expression was repressed (red arrow in Fig. 2F), whereas normal expression was visible in the entire prospective left wing region. These observations are in accordance with the hypothesis that *Tbx5* is involved in early processes before the onset of the Wnt and Fgf protein interaction.

Next, the expression patterns of the same set of markers were examined in the *EnTbx4*-misexpressed embryo. In the *EnTbx4*-misexpressed leg buds, *Wnt8c* expression was repressed in a domain where GFP signals were observed (Fig. 2G,G′). Contrary to this, when *EnTbx4* was misexpressed in the prospective wing, *Wnt2b* was normally expressed, although extensive GFP signals were evident (Fig. 2H,H′). This indicates that *EnTbx4* represses *Wnt8c* in the leg, but not *Wnt2b* in the wing, implying that *EnTbx4* specifically affects *Wnt8c*. *Fgf10* expression was repressed (Fig. 2I), whereas the mesoderm cells on the left side showed normal expression patterns. When the *EnTbx4* construct was electroporated in the leg field, clear repression of *Fgf8* and *Pea3* was evident (red arrowheads in Fig. 2K,L) where robust *Env* expression was observed (Fig. 2J), indicating that *EnTbx4* also abrogates the early processes of limb initiation. In the limbs where the dominant-negative Tbx genes were misexpressed, apoptotic cell death was not detected by the TUNEL method (data not shown).

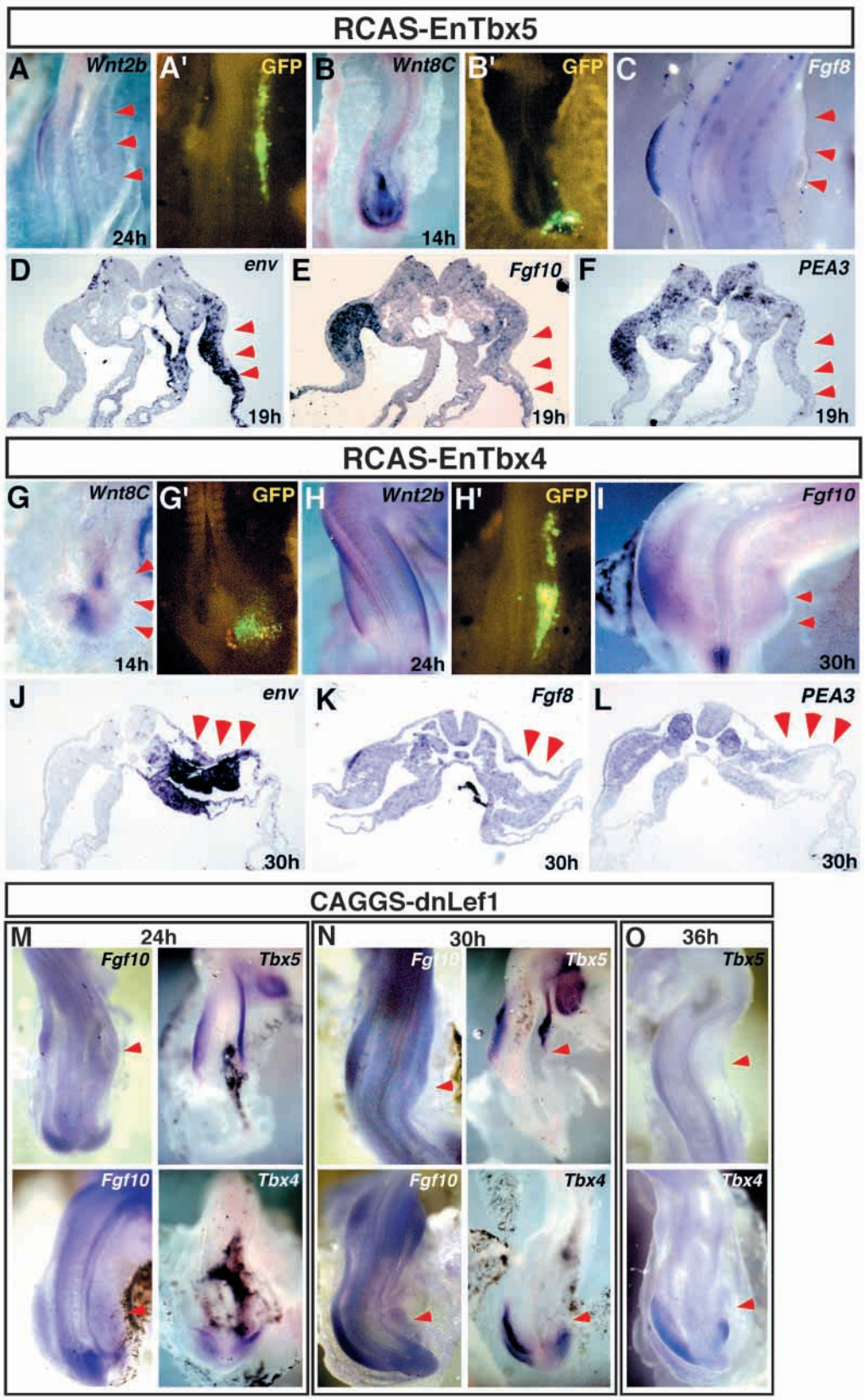

Fig. 2. Expression of the dominant-negative *Tbx5* (*EnTbx5*) and *Tbx4* (*EnTbx4*) induces repression of Wnt and Fgf genes, and *Pea3*. (A) When *EnTbx5* was misexpressed in the prospective wing field by in ovo electroporation, *Wnt2b* expression was repressed 24 hours after electroporation (arrowheads), whereas this gene was normally expressed in the left side. (A′) Robust fluorescent signals derived from the co-electroporated *EGFP* gene were evident where *Wnt2b* was repressed. (B) By contrast, *Wnt8c* expression was normal 14 hours after electroporation of *EnTbx5* in the prospective leg field. (B′) Robust GFP fluorescent signals were observed in the leg field. (C) Expression of *Fgf8* was repressed in the hypoplastic right wing buds (red arrowheads). Normal expression of *Fgf8* was evident in the left wing buds. (D) Robust *Env* expression indicated successful *EnTbx5* misexpression in the prospective wing field 19 hours after electroporation (arrowheads). In such embryos, expression of *Fgf10* (E) and *Pea3* (F) was repressed, whereas the normal expression was evident on the opposite side of the embryo. (G) When *EnTbx4* electroporation was performed in the prospective leg field, *Wnt8c* expression was repressed (arrowheads) where robust GFP signals were observed (G′). (H) When *EnTbx4* was misexpressed in the prospective wing field, *Wnt2b* expression was unaffected, although this area showed strong GFP signals (H′). (I) Expression of *Fgf10* was repressed in the hypoplastic leg buds (red arrowheads). Normal expression of this gene was evident in the left leg buds. (J) Thirty hours after electroporation, robust *env* expression was evident in the leg field (red arrowheads). In its serial sections, expression of *Fgf8* (K) and *Pea3* (L) was repressed (red arrowheads). (M-O) Top row shows wings and bottom row shows legs. Arrowheads indicate repression. (M) When a dominant-negative form of *Lef1* (*dnLef1*) was misexpressed, expression of *Fgf10* was weakly repressed in both *dnLef1*-misexpressed wing and leg fields 24 hours after electroporartion. At this stage, expression of *Tbx5* and *Tbx4* was normal. (N) Repression of *Fgf10* became evident 30 hours after electroporation. At this stage, expression of *Tbx5* and *Tbx4* was also weakly repressed. (O) Repression of *Tbx5* and *Tbx4* became evident 36 hours after electroporation.

Dominant-negative Lef1 does not affect *Tbx5* and *Tbx4* expression

As previously reported, Wnt signaling regulates *Fgf10* expression in both the presumptive wing and leg buds, placing Wnts signaling upstream of *Fgf10* (Kawakami et al., 2001). Although our data suggest that both Tbx5 and Tbx4 control expression of *Wnt2b/Wnt8c*, *Fgf8* and *Fgf10*, misexpression data obtained from the *EnTbx5* and *EnTbx4* constructs do not clarify whether Tbx genes lie upstream of Wnt protein signaling, or vice versa. To elucidate this, an expression construct (CAGGS-*dnLef1*) for a dominant-negative form of *Lef1* (Kengaku et al., 1998), the direct nuclear target of Wnt signaling, was constructed. In this experiment, a pCAGGS vector that has been shown to drive rapid and robust expression of transgenes in tissues was used (Niwa et al., 1991; Koshiba-Takeuchi et al., 2000). This construct was electroporated into both the prospective wing and leg fields at stages 9 to 11, and *Tbx5* and *Tbx4* expression was then examined. Twenty-four hours after electroporation, both *Tbx5* and *Tbx4* were normally expressed in the prospective wing and leg fields, respectively (Fig. 2M). At this stage, *Fgf10* expression was evident in both the wing and leg fields, although weak repression was observed (Fig. 2M). Repression of *Fgf10*, *Tbx5* and *Tbx4* became evident 30 hours after electroporation (Fig. 2N). Thirty-six hours after electroporation, repression of *Tbx5* in the wing and *Tbx4* in the leg became obvious (Fig. 2O). As the Wnt signaling controls *Fgf10* and *Fgf8* expression, we speculate that the *dnLef1* repressed *Fgf10* and *Fgf8*, thereby indirectly downregulating *Tbx5* and *Tbx4* expression. Taken together, our data again suggest that *Tbx5* and *Tbx4* lie upstream of both the Wnt and Fgf signaling in limb induction. In these experiments, pCAGGS-*EGFP* was co-electroporated to visualize the domain of misexpression and GFP signals in the electroporated areas (data not shown).

Tbx5 misexpression in the flank induces an additional wing-like limb

If *Tbx5* and *Tbx4* are involved in the early processes of limb initiation, forced misexpression of these genes in the flank would be expected to induce the formation of additional limb buds, as observed in implantation of Fgf- or Wnt-expressing cells. As *Tbx5* and *Tbx4* specify the wing and leg identity of limb buds, respectively, Tbx5 and Tbx4 misexpression should induce an additional wing and leg, respectively. Chick wing is covered by feathers, whereas leg has scaled digits with claws and feathers in the proximal part. Based upon these morphological differences, we can identify which type of limb is formed by misexpression. Implantation of Wnt-expressing cells, for example, Wnt2b in the restricted flank region, induces a mosaic additional limb (Fig. 3A,A′) with wing-like morphology on the anterior side (W′) and leg-like structure on the posterior (L′) (Fig. 3A′). This additional limb formation is accompanied by the expression of *Tbx5* (red arrow) and *Tbx4* (blue arrow) on the anterior and posterior sides, respectively (Fig. 3B).

To confirm the identity of Wnt2b-induced additional limb buds, we checked expression of Hox9 genes. As reported previously, *Hoxb9* and *Hoxc9* are expressed in the leg, whereas *Hoxd9* is expressed in the wing (Nelson et al., 1996; Cohn et al., 1997; Takeuchi et al., 1999). As expected, leg-specific *Hoxb9* and *Hoxc9* genes were expressed in the posterior side of the additional limbs, leaving the anterior side negative (Fig. 3C,C′). By contrast, wing-specific *Hoxd9* was expressed mainly in the anterior part, although this gene did not show a clear boundary of expression (Fig. 3C″). Consequently, these observations are consistent with the mosaic nature of the Wnt2b-induced additional limbs (Fig. 3D).

For the misexpression experiments, *Tbx5-EGFP* and *Tbx4-EGFP* fusion genes were inserted into the pCAGGS expression vector (CAGGS-*Tbx5-EGFP* and CAGGS-*Tbx4-EGFP*). As previously reported, *Tbx5-EGFP* and *Tbx4-EGFP* fusion genes exhibit the same biological functions as the unmodified *Tbx5* and *Tbx4*, respectively. In addition, the pCAGGS vector drives rapid transgene expression, making this system ideal for analyzing early developmental stages (Niwa et al., 1991; Koshiba-Takeuchi et al., 2000). When the CAGGS-*Tbx5-EGFP* expression construct was electroporated into the flank, a wing-like limb was formed (red arrowhead in Fig. 3E). Although this additional limb is smaller than the normal wing, its digits were extensively covered by feather buds. When this embryo was stained with Alcian Blue, skeletal patterns of this additional wing were similar to the normal wing (data not shown).

When *Wnt2b* expression was examined, induction of this gene was clearly observed in the flank, where the GFP was evident (Fig. 3F,G). *Fgf10* gene was induced in the small additional limb bud (red arrowhead in Fig. 3H). Sixty hours after electroporation, an additional limb was clearly observed at the posterior side of the normal wing (red arrowhead in Fig. 3I). In this additional limb, distinct expression of *Fgf8* was detected in the AER (red arrowhead in Fig. 3I).

To confirm the wing identity of this additional limb, we checked expression of Hox9 genes. In the additional limb, expression of leg-specific *Hoxb9* was observed only in the posterior margin (Fig. 3J). Expression of another leg-specific *Hoxc9* became very faint (Fig. 3K). By contrast, wing-specific *Hoxd9* was expressed (Fig. 3L). These results indicate that the Tbx5-induced additional limb predominantly possesses the wing identity, with the wing-like expression of *Hox9* genes, albeit partially.

Tbx4 misexpression in the flank induces an additional leg-like limb

When the expression plasmid CAGGS-*Tbx4-EGFP* was electroporated into the flank at stage 10, an additional limb was induced at E10 (red arrowheads in Fig. 3M). Contrary to the Tbx5 misexpression, this limb showed leg-like morphology in its distal half: separated digits were covered by scales, and claw formation on the digit tips and suppression of feather formation were evident in the distal part (Fig. 3M). Unlike the Wnt2b-induced additional limb (Fig. 3A,A′), this additional limb has a leg-like appearance on both the anterior and posterior sides, despite its proximal region showing wing-like morphology. When the expression of several markers was examined, *Wnt8c* induction was evident (Fig. 3N) in an area where EGFP was observed (Fig. 3O). *Fgf10* and *Fgf8* were induced in the electroporated parts (Fig. 3P,Q, respectively). Collectively, these data indicate that *Tbx5* and *Tbx4* act at the early stages of limb initiation, controlling the downstream Wnt and Fgf signaling cascades.

When expression of Hox9 genes was examined, leg-specific *Hoxb9* and *Hoxc9* genes were induced in this additional limb (Fig. 3R,S, respectively). By contrast, expression of wing-specific *Hoxd9* was suppressed, especially in the posterior half.

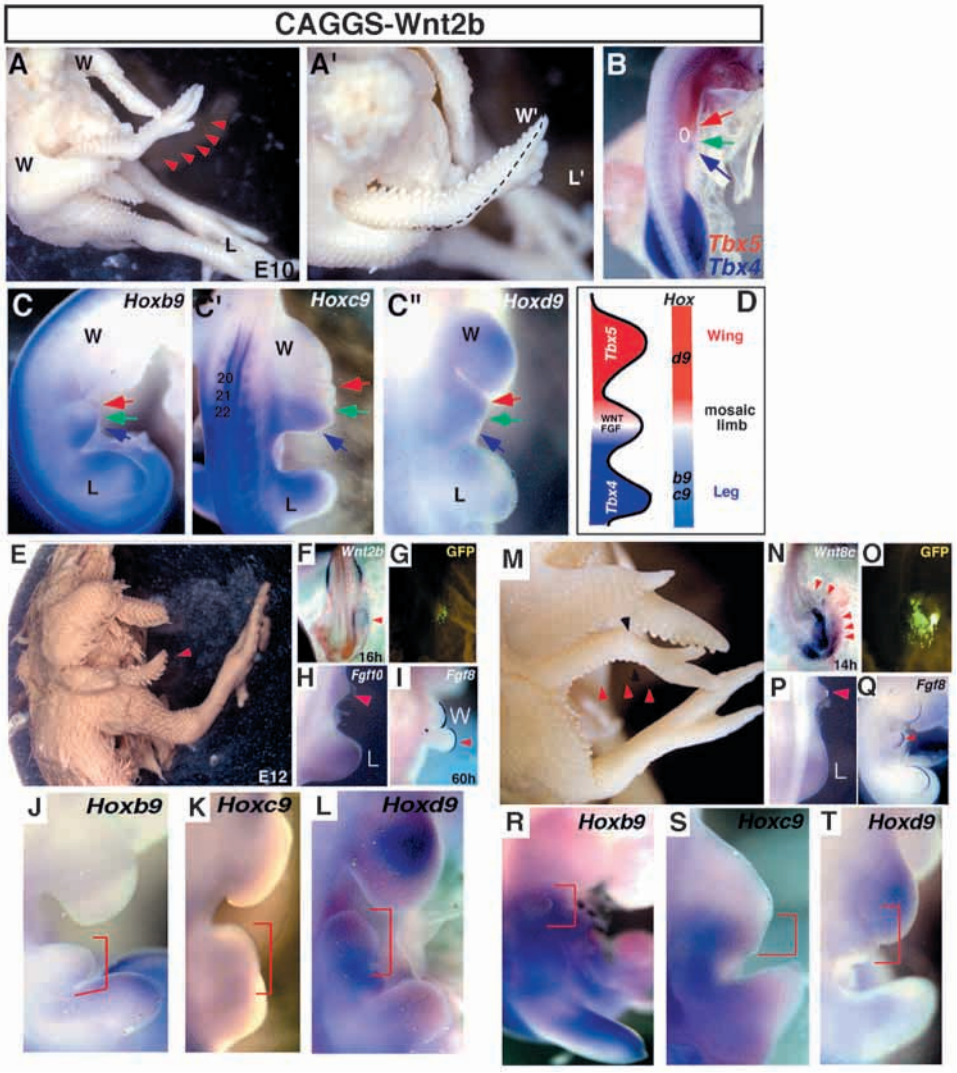

Fig. 3. Additional limb formation induced by *Wnt2b*, *Tbx5* and *Tbx4* in the flank. (A) When *Wnt2b*-expressing cells were implanted in the flank, a mosaic limb was formed (red arrowheads). (A′) Careful examination of this additional limb revealed its mosaic structures with wing-like morphology on the anterior side (W′) and leg-like structure on the posterior side (L′). (B) At earlier stages, the Wnt2b-induced additional limb (green arrow) expressed *Tbx5* (red arrow) and *Tbx4* (blue arrow) in its anterior and posterior sides, respectively. A white circle indicates the position of cell implantation. (C to C″) In the Wnt2b-induced limb buds, leg-specific *Hoxb9* (C) and *Hoxc9* (C′) were expressed in the posterior region, whereas wing-specific *Hoxd9* (C″) in the anterior. Arrows correspond to the positions indicated in B. (D) Schematic representation of the Wnt- or Fgf-induced additional limb and its mosaic structures. (E) When CAGGS-*Tbx5-EGFP* plasmid was electroporated in the flank, wing-like limb was formed (red arrowhead), covered extensively by feather buds. (F) About 16 hours after electroporation, *Wnt2b* expression was induced (arrowhead) in the electroporated area visualized by the GFP (G). Expression of *Fgf10* (H) was observed in the induced limb bud (red arrowhead). L, normal leg bud. (I) About 60 hours after electroporation, an additional limb (red arrowhead) was formed at the caudal side of the normal wing (W). This additional limb bud expressed *Fgf8* in the AER (red arrowhead). (J) In the Tbx5-induced limb, expression of leg-specific *Hoxb9* was observed weakly only in the posterior margin, excluded form the anterior part of limb. (K) Expression of another leg-specific *Hoxc9* was very faint. (L) By contrast, wing-specific *Hoxd9* was expressed. Red brackets indicate additional limbs. (M) When the CAGGS-*Tbx4-EGFP* plasmid was electroporated in the flank, a leg-like limb was formed (red arrowheads). Black arrowheads indicate a boundary between feather and scale domains. When expression of several marker genes was examined, *Wnt8c* (N, red arrowheads) was induced. Electroporation was monitored by the GFP as shown in O. (P) Likewise, expression of *Fgf10* was induced in the additional limb bud (red arrowhead). (Q) In the *Tbx4*-induced limb bud, expression of *Fgf8* (red arrowhead) was observed in the AER. In the additional limb buds, leg-specific *Hoxb9* (R) and *Hoxc9* (S) were expressed. (T) By contrast, expression of wing-specific *Hoxd9* was suppressed, although faint expression was observed at the anterior margin. Red brackets indicate additional limbs.

(Fig. 3T). These results suggest that the Tbx4-induced additional limb mainly possesses the leg identity, with partial wing-like appearance.

Stage-dependent action of *Tbx5* and *Tbx4*

As observed in Table 1, the actions of dominant-negative Tbx genes and the resultant phenotypes are dependent on the developmental stages, where stages 7 to 10 are highly susceptible phases. To complement these loss-of-function approaches, stage-dependent actions of *Tbx5* and *Tbx4* in gain-of-function experiments were examined. For this purpose, we electroporated pCAGGS-*Tbx5-EGFP* and pCAGGS-*Tbx4-EGFP* plasmids at various stages (summarized in Table 2). Interestingly, in both cases, induction of additional limb formation was obtained only when these expression plasmids were electroporated between stages 8 and 12. From stage 13 onwards, complete induction of additional limb formation was never observed, although we observed robust fluorescent signal derived co-electroporated pCAGGS-*EGFP* (data not shown). This is in clear contrast to the Fgf-induced additional limb buds in the flank, which can be induced when Fgf is applied during stages 13 to 15 (Crossley et al., 1996; Vogel et al., 1996). Local application of Fgf at earlier or later stages never induces additional limb buds, setting up a brief sensitive window. This also suggests that competence to the Fgf signaling is strictly controlled in a stage-dependent way. Contrary to this, our misexpression experiments have shown that the formation of additional limb buds is observed only when Tbx genes are

misexpressed in the flank between stages 8 and 12, before the mesoderm cells become competent to respond to Fgf signaling. Thus, the Tbx-sensitive period begins and ends before the stages at which Wnt-expressing cells can induce additional limb buds. These lines of evidence again indicate that *Tbx5* and *Tbx4* act upstream of Wnt/Fgf signaling (Fig. 4).

DISCUSSION

In vertebrates, a correct pattern of organ formation is crucially dependent on interactions between different embryonic tissues. For initiation of limb outgrowth, two different inductive signals, Fgf and Wnt, establish tight regulatory loops to ensure the correct transduction of signals and morphogenesis (Kawakami et al., 2001). Prior to limb initiation, *Wnt2b* is expressed in the intermediate and the lateral plate mesoderm of the prospective wing field. In the prospective leg region, *Wnt8c* is expressed in the caudal region of the lateral plate mesoderm. Through a β-catenin-dependent pathway, these Wnt molecules induce *Fgf10* in the prospective wing and leg fields. Consequently, Fgf10 induces *Fgf8* in the surface ectoderm through the Wnt3a/β-catenin-dependent pathway. Hence, orchestrated influx and efflux of morphogenetic signals between different embryonic tissues are pivotal for the correct pattern formation of vertebrate limb buds. As reported previously, *Tbx5* and *Tbx4* genes are activated in Fgf-induced ectopic limbs in the flank (Ohuchi et al., 1998; Gibson-Brown et al., 1998; Issac et al., 1998; Logan et al., 1998). Our study has shown that Tbx genes induce Fgf genes in the flank, suggesting that the influx and efflux of signals operate in the Tbx/Fgf cascade.

When the dominant-negative forms of *Tbx5* and *Tbx4* were misexpressed in the prospective limb fields, complete limbless phenotypes arose with disruption of shoulder and pelvis formation (Fig. 1). Scapula was not formed, and ribs were hypomorphic. In the leg region, ilium and ischium were hypoplastic without pubis formation, implying that scapula is part of the limb. These results indicate that suppression of functions of Tbx genes affect not only the limb development, but also the formation of shoulder and pelvis. Similar morphological alterations were observed in the *Fgf10*-knockout mouse (Sekine et al., 1999; Min et al., 1998). In such mutant limbless mouse, posterior scapula was missing and iliac bone was rudimentary. As miexpression of the dominant-negative Tbx genes represses the expression of *Fgf10* and *Fgf8*, morphological changes observed in chick and mouse are alike. Nonetheless, induced alterations were severer in chick embryos, probably because the dominant-negative Tbx genes affect both the Wnt and Fgf cascades.

To construct the dominant-negative forms of Tbx genes, we used the *Engrailed* suppressor domain. It has been reported that the repressor activity of this domain is mediated through the interaction with Groucho (Jimenez et al., 1997; Tolkunova et al., 1998). Although vertebrate *Groucho*-related genes are widely expressed in developing embryos (Fisher and Caudy, 1998; Chen and Courey, 2000), their activities in the limb are unclear. Nonetheless, when analyzed in primary cultures of chick limb mesenchyme cells, both *EnTbx5* and *EnTbx4* abrogate efficiently the transcriptional activation of the *Anf* and *Fgf10* promoters by Tbx5 and Tbx4, respectively (data

Table 2. Stage-dependent actions of *Tbx5* and *Tbx4* in limb initiation

A Effect of *CAGGS-Tbx5*

Stage of injection	Total	Number of wing-like extra limbs
8	8	0 (15%)
9	15	2 (13%)
10	14	7 (50%)
11	15	7 (47%)
12	15	1 (7%)
13	13	0 (0%)
14	10	0 (0%)
15	8	0 (0%)
Totals	103	19

B Effect of *CAGGS-Tbx4*

Stage of injection	Total	Number of leg-like extra limbs
8	8	0 (0%)
9	15	4 (27%)
10	12	5 (42%)
11	18	6 (33%)
12	16	2 (13%)
13	12	0 (0%)
14	10	0 (0%)
15	10	0 (0%)
Totals	92	17

(A) *Tbx5* was misexpressed by in ovo electroporation at various developmental stages. Wing-like additional limbs were induced only when electroporation was performed at stages 8 to 12.

(B) Likewise, formation of leg-like additional limbs was observed only when *Tbx4* was misexpressed at stages 9 to 12, setting up a short critical period from stages 8 to 12.

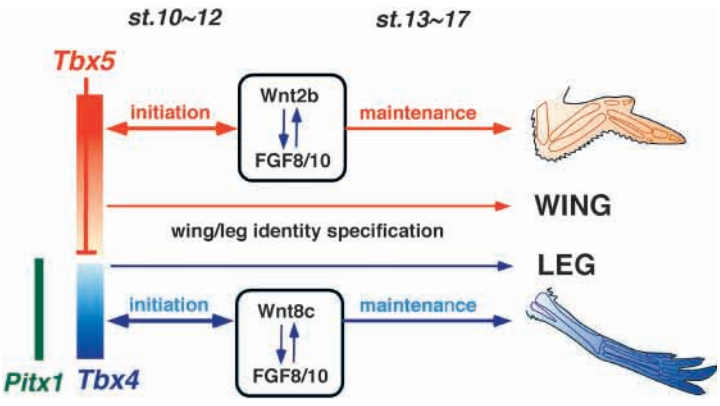

Fig. 4. Schematic representation of the signal cascade. In early stages of limb development (stages 10 to 12), *Tbx5* and *Tbx4* activate the Wnt2B/Fgf and Wnt8C/Fgf signals, respectively. Once activated, the Wnt/Fgf cascades feedback on to *Tbx5* and *Tbx4* genes to establish a tight positive regulatory loop. At later developmental stages, the Wnt and Fgf signaling cascades interact to make a positive feedback loop and maintain outgrowth of limb buds. During later stages, *Tbx5* and *Tbx4* exert distinct actions to make different limb structures: wing and leg, respectively.

not shown). This suggests that the Engrailed acts as an efficient suppressor in the chick limb buds. Recently, it has been reported that functional knockdown of zebrafish *tbx5* resulted in a failure of fin bud initiation and the complete loss of pectoral fins (Ahn et al., 2002), indicating that the antisense oligonucleotide-mediated knockdown and misexpression of *EnTbx5* resulted in similar morphological alterations. Hence, exploiting different techniques in different species is important to understand the common mechanism of limb initiation.

Although the extracellular events have been analyzed extensively, intracellular mechanisms that regulate gene expression and limb initiation have remained unsolved. To date, Hox9 genes are known to be expressed in the lateral plate mesoderm. Expression of these genes demarcates the fields of both the normal limb and the additional limbs induced in the flank. This indicates that Hox genes act upstream of these signaling molecules (Cohn et al., 1997). However, a gap exists between the Hox genes and the Wnt/Fgf network. Our data strongly indicate that *Tbx5* and *Tbx4* operate in this gap. We also have shown that Hox9 genes are controlled by *Tbx5* and *Tbx4* during wing/leg specification (Takeuchi et al., 1999). These lines of evidence suggest that a regulatory loop between Hox9 and Tbx genes is essential for both limb initiation and the wing/leg identity specification, highlighting the feedback and feed-forward mechanisms in both extracellular and intracellular signaling cascades.

As shown in Fig. 3, misexpression of Tbx5 and Tbx4 in the flank induces wing-like and leg-like limbs, respectively. Nonetheless, these additional limbs did not show the complete wing or leg appearance. Rather, Tbx5- and Tbx4-induced limbs seem to be mosaic with one type predominating over another. This is consistent with the mixed expression patterns of Hox9 genes (Fig. 3). To obtain rapid and robust expression of Tbx genes, we used pCAGGS expression vector. As pCAGGS induces transient expression of transgene, expression of Tbx genes in the flank might have faded out after triggering expression of Wnt/Fgf genes. This would suggest that induced Wnt/Fgf proteins might initiate limb formation even in mesenchyme cells that were not electroporated. In such case, additional limb buds can be composed of mixed cell populations; electroporated Tbx-positive cells and non-electroporated Tbx-negative cells thereby have a mosaic appearance.

Tbx genes regulate pattern formation in both vertebrate and invertebrate embryos. From a combination of embryological and genetic approaches, a picture is emerging that Tbx genes belong to a highly conserved genetic network involving inductive signals (Papaioannou and Silver, 1998; Smith, 1999; Ruvinsky and Gibson-Brown, 2000; Tada and Smith, 2001). In *Xenopus*, another T-box transcription factor, Brachyury (Xbra), directly regulates *embryonic fibroblast growth factor* (*eFgf*) and creates a tight feedback loop. Hence, eFgf expression maintains *Xbra* expression, and Xbra maintains *eFgf* expression in vivo. Conversely, *eFgf* inhibition represses *Xbra* expression and *Xbra* inhibition represses *eFgf* expression (Isaacs et al., 1994). In addition, *Xbra* has been found to regulate the *Xenopus Wnt11* gene directly, making another connection to Wnt signaling (Tada and Smith, 2000). In *Drosophila*, functions of T-box transcription factor *optomotor blind* (*omb*) are closely related to Dpp (Decapentaplegic) and Wg (Wingless) signaling cascades. (Pflugfelder et al., 1992; Maves and Schubiger, 1998). These observations strongly suggest that Tbx genes are central in the highly conserved signaling cascades of these inductive signals in both vertebrates and invertebrates.

Although our data indicate that *Tbx5* and *Tbx4* control Wnt and Fgf genes, how these signals are transduced to the nucleus to control expression of target genes remains to be elucidated. In this sense, we do not exclude the possibility that Tbx proteins act cooperatively with the Wnt and Fgf signaling systems, i.e. in parallel or cooperatively with these cascades. This is compatible with the data published previously (Ng et al., 2002). Because another T-box protein, Tbr1, interacts with CASK, a member of the membrane-associated guanylate kinases (MAGUKs) (Hsueh et al., 2000), Tbx proteins may be targets of extracellular signaling that could change their transcriptional properties depending on the signaling context. This could be related to the stage-dependent action of Tbx genes during limb initiation. As described above, induction of additional limb formation was obtained only when Tbx genes were electroporated between stages 8 and 12. This is in clear contrast to the Fgf-induced additional limb buds in the flank, which can be induced when Fgf is applied during stages 13 to 15 (Crossley et al., 1996; Vogel et al., 1996; Ohuchi et al., 1997; Kawakami et al., 2001). This also strongly suggests that competence to the Tbx misexpression and to the Fgf signaling is strictly controlled in a stage-dependent way. Although we do not know how these differences in the competence are controlled in vivo, the signaling context could modulate Tbx proteins and regulate this critical factor during limb development.

Recently, *Anf* was shown to be a direct target of *Tbx5* (Hiroi et al., 2001; Bruneau et al., 2001). Tbx5 alone activates the *Anf* promoter efficiently. However, in the presence of another transcription factor, *Nkx2.5*, *Tbx5* is a stronger activator. In the early stages of limb initiation, Tbx5 alone could induce Wnt genes, whereas in the later stages, activated Wnt signaling might modulate *Tbx5* activity or induce another transcription factor to act synergistically, forming a positive feedback loop and upregulating *Fgf10* to maintain limb outgrowth. To examine this hypothesis, precise biochemical analyses needs to be performed.

Our data reveal that *Tbx5* and *Tbx4* specifically regulate *Wnt2b* and *Wnt8c*, respectively, to initiate limb outgrowth in the early stages of development. In the later stages, *Tbx5* and *Tbx4* exert different actions to form distinct forelimb and hindlimb structures, respectively. These indicate that these genes play distinct roles with distinct specificity. Nonetheless, *Tbx5* and *Tbx4* are derived from the same ancestral gene (Agulnik et al., 1996; Ruvinsky and Silver, 1997). During evolution, these genes have diversified their biological functions to regulate different Wnt genes and make different limb structures. This is related to our observation that *EnTbx5* and *EnTbx4* failed to repress *Wnt8c* in the leg and *Wnt2b* in the wing. As expected, misexpression of *EnTbx5* in the leg and *EnTbx4* in the wing did not affect limb development (Fig. 1E,F). This suggests that Tbx5 and Tbx4 have acquired different target specificities during evolution. Although we are still far from a complete understanding of these processes, our data shed further light on vertebrate limb evolution of vertebrate limbs, the functions and evolution of the Tbx gene family.

We thank Drs Benoit Bruneau, Juan Carlos Izpisua-Belmonte, Malcolm P. Logan and Cliff Tabin for sharing unpublished data prior to publication. We also thank Dr Shinichi Nakagawa for Wnt2b and Lef1 constructs, Dr Benoit Bruneau for mouse *Fgf10* promoter luciferase reporter construct and Dr Cheryll Tickle for critical comments on the manuscript. This work was supported by a Grant-in-Aids for Scientific Research on Priority Areas (C) and Creative Basic Research from the Ministry of Education, Science Sports and Culture of Japan (T.O.) and the Toray Science Foundation (T.O.). This work was also funded in part by the Inoue Foundation for Science (J.K.T). J.K.T is supported by JSPS Research Fellowships for Young Scientists.

REFERENCES

Agulnik, S. I., Garvey, N., Hancock, S., Ruvinsky, I., Chapman, D. L., Agulnik, I., Bollag, R., Papaioannou, V. and Silver, L. M. (1996). Evolution of mouse T-box genes by tandem duplication and cluster dispersion. *Genetics* **144**, 249-254.

Ahn, D. G., Kourakis, M. J., Rohde, L. A., Silver, L. M. and Ho, R. K. (2002). T-box gene *tbx5* is essential for formation of the pectoral limb bud. *Nature.* **417**, 754-758.

Bruneau, B. G., Nemer, G., Schmitt, J. P., Charron, F., Robitaille, L., Caron, S., Conner, D. A., Gessler, M., Nemer, M., Seidman, C. E. and Seidman, J. G. (2001). A murine model of Holt-Oram syndrome defines roles of the T-box transcription factor Tbx5 in cardiogenesis and disease. *Cell* **106**, 709-721.

Chapman, D. L., Garvey, N., Hancock, S., Alexiou, M., Agulnik, S. I., Gibson-Brown, J. J., Cebra-Thomas, J., Bolag, R. J., Siver, L. M. and Papaioannou, V. E. (1996). Expression of the T-box Family Genes, TBX1-TBX5, During Early Mouse Development. *Dev. Dyn.* **206**, 379-390.

Chen, G. and Courey, A. J. (2000). Groucho/TLE family proteins and transcriptional repression. *Gene* **249**, 1-16.

Cohn, M. J., Izpisua-Belmonte, J. C., Abud, H., Heath, J. K. and Tickle, C. (1995). Fibroblast growth factors induce additional limb development from the flank of chick embryos. *Cell* **80**, 739-746.

Cohn, M. J., Patel, K., Krumlauf, R., Wilkinson, D. G., Clarke, J. D. and Tickle, C. (1997). Hox9 genes and vertebrate limb specification. *Nature* **387**, 97-101.

Crossley, P. H., Minowada, G., MacArthur, C. A. and Martin, G. R. (1996). Roles for FGF8 in the induction, initiation, and maintenance of chick limb bud development. *Cell* **84**, 127-136.

Fisher, A. L. and Caudy, M. (1998). Groucho proteins: transcriptional corepressors for specific subsets of DNA-binding transcription factors in vertebrates and invertebrates. *Genes Dev.* **12**, 1931-1940.

Gibson-Brown, J. J., Agulnik, S., Chapman, D., Alexiou, M., Garvey, N., Silver, L. and Papaioannou, V. (1996). Evidence for a role for T-box genes in the evolution of limb morphogenesis and the specification of forelimb/hindlimb identity. *Mech Dev.* **56**, 93-101.

Gibson-Brown, J. J., Agulnik, S. I., Silver, L. M., Niswander, L. and Papaioannou, V. (1998). Involvement of T-box genes Tbx2-Tbx5 in vertebrate limb specification and development. *Development* **125**, 2499-2509.

Hamburger, V. and Hamilton, H. L. (1951). A series of normal stages in the development of the chick embryo. *J. Morphol.* **88**, 49-92.

Hiroi, Y., Kudoh, S., Monzen, K., Ikeda, Y., Yazaki, Y., Nagai, R. and Komuro, I. (2001). Tbx5 associates with Nkx2-5 and synergistically promotes cardiomyocyte differentiation. *Nat Genet.* **28**, 276-280.

Hsueh, Y. P., Wang, T. F., Yang, F. C. and Sheng, M. (2000). Nuclear translocation and transcription regulation by the membrane-associated guanylate kinase CASK/LIN-2. *Nature* **404**, 298-302.

Hume, C. R. and Dodd, J. (1993). Cwnt-8C: a novel Wnt gene with a potential role in primitive streak formation and hindbrain organization. *Development* **119**, 1147-1160.

Isaacs, H. V., Pownall, M. E. and Slack, J. M. (1994). eFGF regulates *Xbra* expression during Xenopus gastrulation. *EMBO J.* **13**, 4469-4481.

Issac, A., Rodriguez-Esteban, C., Ryan, A., Altabef, M., Tsukui, T., Patel, K., Tickle, C. and Izpisua-Belmonte, J. C. (1998). Tbx genes and limb identity in chick embryo development. *Development* **125**, 1867-1875.

Jaynes, J. B. and O'Farrell, P. H. (1991). Active repression of transcription by the engrailed homeodomain protein. *EMBO J.* **10**, 1427-1433.

Jimenez, G., Paroush, Z. and Ish-Horowicz, D. (1997). Groucho acts as a corepressor for a subset of negative regulators, including Hairy and Engrailed. *Genes Dev.* **11**, 3072-3082.

Kawakami, Y., Capdevila, J., Buscher, D., Itoh, T., Rodriguez-Esteban, C. and Izpisua-Belmonte, J. C. (2001). WNT signals control FGF-dependent limb initiation and AER induction in the chick embryo. *Cell* **104**, 891-900.

Kengaku, M., Capdevila, J., Rodrigues-Esteban, C., de la Pena, J., Johnson, R. L., Belmonte, J. C. and Tabin, C. J. (1998). Distinct WNT pathways regulating AER formation and dorsoventral polarity in the chick limb bud. *Science* **280**, 1274-1277.

Kispert, A. and Herrmann, B. G. (1993). The *Brachyury* gene encodes a novel DNA binding protein. *EMBO J.* **12**, 3211-3220.

Koshiba-Takeuchi, K., Takeuchi, J. K., Matsumoto, K., Momose, T., Uno, K., Hoepker, V., Ogura, K., Takahashi, N., Nakamura, H. and Yasuda, K. (2000). Tbx5 and retinotectum projection. *Science* **287**, 134-137.

Logan, M., Simon, H. G. and Tabin, C. (1998). Differential regulation of T-box and homeobox transcription factors suggests roles in controlling chick limb-type identity. *Development* **125**, 2825-2835.

Martin, G. R. (1998). The roles of FGFs in the early development of vertebrate limbs. *Genes Dev.* **12**, 1571-1586.

Martin, G. R. (2001). Making a vertebrate limb: New players enter from the wings. *BioEssays* **23**, 865-868.

Maves, L. and Schubiger, G. (1998). A molecular basis for transdetermination in Drosophila imaginal discs: interactions between wingless and decapentaplegic signaling. *Development* **125**, 115-124.

Min, H., Danilenko, D. M., Scully, S. A., Bolon, B., Ring, B. D., Tarpley, J. E., DeRose, M. and Simonet, W. S. (1998). *Fgf-10* is required for both limb and lung development and exhibits striking functional similarity to *Drosophila* branchless. *Genes Dev.* **12**, 3156-3161.

Mogan, B. A. and Fekete, D. M. (1996). Manipulating gene expression with replication-competent retroviruses. *Methods Cell Biol.* **51**, 185-218.

Momose, T., Tonegawa, A., Takeuchi, J., Ogawa, H., Umesono, K. and Yasuda, K. (1999). Efficient targeting of gene expression in chick embryos by microelectroporation. *Dev. Growth Differ.* **41**, 335-344.

Muller, C. and Herrmann, B. G. (1997). Crystallographic structure of the T domain-DNA complex of the Brachyury transcription factor. *Nature* **389**, 884-888.

Nelson, C. E., Morgan, B. A., Burke, A. C., Laufer, E., DiMambro, E., Murtaugh, L. C., Gonzales, E., Tessarollo, L., Parada, L. F. and Tabin, C. (1996). Analysis of Hox gene expression in the chick limb bud. *Development* **122**, 1449-1466.

Ng, J. K., Kawakami, Y., Buscher, D., Raya, A., Itoh, T., Koth, C. M., Rodriguez Esteban, C., Rodriguez-Leon, J., Garrity, D. M., Fishman, M. C. and Izpisua Belmonte, J. C. (2002). The limb identity gene Tbx5 promotes limb initiation by interacting with Wnt2b and Fgf10. *Development* **129**, 5161-5170.

Niswander, L., Jeffrey, S., Martin, G. and Tickle, C. (1994). A positive feedback loop coordinates growth and patterning in the limb. *Nature* **371**, 609-612.

Niwa, H., Yamamura, K. and Miyazaki, J. (1991). Efficient selection for high-expression transfectants with a novel eukaryotic vector. *Gene* **108**, 193-199.

Ohuchi, H., Nakagawa, T., Yamauchi, M., Ohata, T., Yoshioka, H., Kuwana, T., Mima, T., Mikawa, T., Nohno, T. and Noji, S. (1995). An additional limb can be induced from the flank of the chick embryo by FGF4. *Biochem. Biophys. Res. Commun.* **209**, 809-816.

Ohuchi, H., Nakagawa, T., Yamamoto, A., Araga, A., Ohata, T., Ishimaru, Y., Yoshioka, H., Kuwana, T., Nohno, T., Yamasaki, M., Itoh, N. and Noji, S. (1997). The mesenchymal factor, FGF10, initiates and maintains the outgrowth of the chick limb bud through interaction with FGF8, an apical ectodermal factor. *Development* **124**, 2235-2244.

Ohuchi, H., Takeuchi, J., Yoshioka, H., Ishimaru, Y., Ogura, K., Takahashi, N., Ogura, T. and Noji, S. (1998). Correlation of wing-leg identity in ectopic FGF-induced chimeric limbs with the differential expression of chick Tbx5 and Tbx4. *Development* **125**, 51-60.

Papaioannou, V. E. and Silver, L. M. (1998). The T-box gene family. *BioEssays* **20**, 9-19.

Pflugfelder, G. O., Roth, H., Poeck, B., Kerscher, S., Schwarz, H., Jonschker, B. and Heisenberg, M. (1992). The *lethal(1)optomotor-blind* gene of *Drosophila melanogaster* is a major organizer of optic lobe development: isolation and characterization of the gene. *Proc. Natl. Acad. Sci. USA* **89**, 1199-1203.

Raible, F. and Brand, M. (2001). Tight transcriptional control of the ETS domain factors Erm and Pea3 by Fgf signaling during early zebrafish development. *Mech. Dev.* **107**, 105-117.

Rodrigues-Esteban, C., Tsukui, T., Yonei, S., Magallon, J., Tamura, K. and Izpisua-Belmonte, J. C. (1999). The T-box genes *Tbx4* and *Tbx5* regulate limb outgrowth and identity. *Nature* **398**, 814-818.

Roehl, H. and Nusslein-Volhard, C. (2001). Zebrafish pea3 and erm are general targets of FGF8 signaling. *Curr. Biol.* **11**, 503-507.

Ruvinsky, I. and Silver, L. M. (1997). Newly identified paralogous groups on mouse chromosomes 5 and 11 reveal the age of a T-Box cluster duplication. *Genomics* **40**, 262-266.

Ruvinsky, I. and Gibson-Brown, J. J. (2000). Genetic and developmental bases of serial homology in vertebrate limb evolution. *Development* **127**, 5233-5244.

Schutte, B. C., Ranade, K., Pruessner, J. and Dracopoli, N. (1997). Optimized conditions for cloning PCR products into an XcmI T-vector. *BioTechniques* **22**, 40-42.

Sekine, K., Ohuchi, H., Fujiwara, M., Yamasaki, M., Yoshizawa, T., Sato, T., Yagishita, N., Matsui, D., Koga, Y., Itoh, N. and Kato, S. (1999). *Fgf10* is essential for limb and lung formation. *Nat. Genet.* **21**, 138-141.

Smith, J. C. (1999). T-box genes: what they do and how they do it. *Trends Genet.* **15**, 154-158.

Tada, M. and Smith, J. C. (2000). Xwnt11 is a target of xenopus brachyury: regulation of gastrulation movements via dishevelled, but not through the canonical wnt pathway. *Development* **127**, 2227-2238.

Tada, M. and Smith, J. C. (2001). T-targets: Clues to understanding the functions of T-box proteins. *Dev. Growth Differ.* **43**, 1-11.

Takeuchi, J. K., Koshiba-Takeuchi, K., Matsumoto, K., Vogel-Hopker, A., Naitoh-Matsuo, M., Ogura, K., Takahashi, N., Yasuda, K. and Ogura, T. (1999). *Tbx5* and *Tbx4* genes determine the wing/leg identity of limb buds. *Nature* **398**, 810-814.

Tolkunova, E. N., Fujioka, M., Kobayashi, M., Deka, D. and Jaynes, J. B. (1998). Two distinct types of repression domain in engrailed: one interacts with the groucho corepressor and is preferentially active on integrated target genes. *Mol Cell Biol.* **18**, 2804-2814.

Vogel, A., Rodriguez, C. and Izpisua-Belmonte, J. C. (1996). Involvement of FGF-8 in initiation, outgrowth and patterning of the vertebrate limb. *Development* **122**, 1737-1750.

Wikinson, D. G. (1993). Whole mount in situ hybridization of vertebrate embryos. In *In Situ Hybridization*, pp. 75-83. New York: Oxford University Press.